FUDMA Journal of Engineering and Technology
ISSN: 3092-9385
https://fjet.fudutsinma.edu.ng/index.php/fjet/
Volume 2, Issue 1, 2026, 1063-1082

Design and Simulation of a 200 MWp Floating Solar PV Plant Integrated with the Kainji Hydropower Plant, Nigeria

Umar A. ADAMU[1*], Ya'u S. HARUNA[2], Ganiyu A. BAKARE[3], Buhari H. MAMMAN[4], Kunduli MUSTAPHA[5], Hadi M. ADAMU[6], Ismaila MAHMUD[7]

[1*,2,3,4]Department of Electrical and Electronics Engineering, Abubakar Tafawa Balewa University, Bauchi, Nigeria
[5]Department of Electrical and Electronics Engineering, University of Maiduguri, Maiduguri, Nigeria
[6]Department of Electrical and Electronics Technology Education, Kaduna Polytechnic, Kaduna, Nigeria
[7]Department of Electrical Engineering, Ahmadu Bello University Zaria, Nigeria

[1*]umaratbu@gmail.com, [2]ysharuna@atbu.edu.ng, [3]gabakare@atbu.edu.ng, [4]bmhassan@atbu.edu.ng, [5]kunduli@unimaid.edu.ng, [6]hadimaikusa@gmail.com, [7]imahmud@abu.edu.ng

Abstract
Nigeria continues to experience persistent electricity generation deficits despite its abundant renewable energy resources. This study presents the design and simulation of a 200 MWp Floating Solar Photovoltaic (FSPV) plant integrated with the 760 MW Kainji Hydropower Plant as a hybrid renewable energy solution for improving grid reliability and renewable energy penetration. Meteorological, hydrological, and geographical data of the Kainji reservoir were analysed. PV system sizing and energy yield simulations were carried out using PVsyst, while floating platform structures, pontoons, anchors, and mooring systems were modelled using SketchUp. The results showed that the system required 333,340 monocrystalline PV modules rated at 600 W each, installed at an optimal tilt angle of 12°, supported by approximately 4.0 million pontoons (12 pontoons per module), occupying about 1.01 km² of reservoir surface area—only 2.7% of the feasible reservoir area. The proposed plant achieves an annual energy yield of approximately 322.1 GWh at P50 (i.e., 50 % probability of exceedance), with a performance ratio of 77.97% and a capacity factor of 18%. The hybrid configuration leveraged the existing 330 kV transmission infrastructure and allowed hydropower to act as virtual energy storage, improving dispatch flexibility and grid stability. The study confirms the technical feasibility of large-scale FSPV deployment in Nigeria and provides a practical framework for integrating floating solar with existing hydropower assets.

Keywords: Floating Solar Photovoltaic, Hybrid Renewable Energy System, Kainji Dam, PVsyst, Grid Stability.

1.0 Introduction

Nigeria's electricity provision remains deeply inadequate relative to national requirements, even though the country possesses an installed generation capacity exceeding 13,000 MW. Actual available generation typically falls between 3,500 MW and 5,500 MW, while estimated demand stands at roughly 20,000 MW [1]. This gap forces widespread reliance on fossil-fuel generators and leads to persistent grid instability. Hydropower contributes approximately 25% of the national generation mix, but its output is heavily influenced by seasonal water availability, reservoir siltation, and aging equipment, causing reduced production during dry periods. The rest of the grid supply comes mainly from natural-gas-fired thermal plants, which suffer from fuel supply constraints and operational inefficiencies [2]. Figure 1 shows the projected peak load demand for Nigeria through 2035 [3].

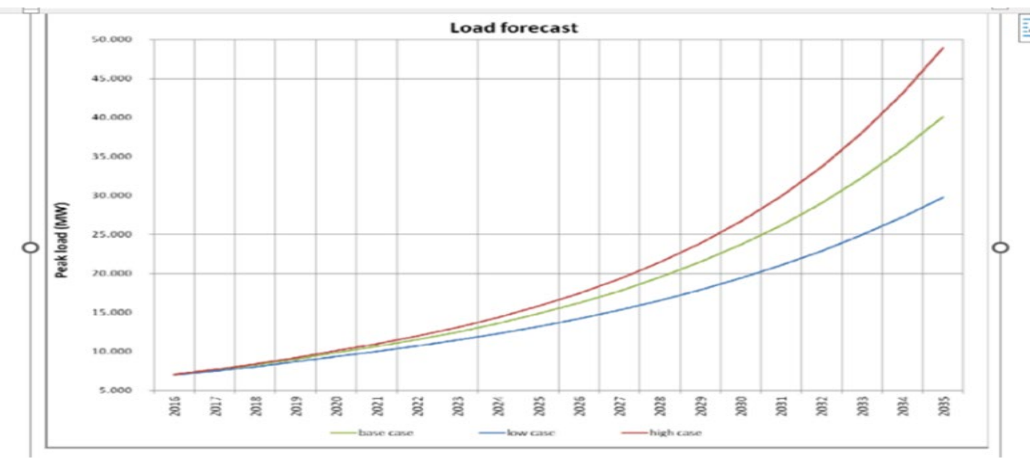

Figure 1: National Peak Load Demand Forecast for Nigeria [3]

Received: 17/05/2026; Revised: 23/05/2026; Accepted: 02/06/2026; Published: 27/06/2026

Figure 1 clearly illustrates that electricity demand is rising rapidly, widening the generation deficit. In 2026, the current available generation of about 5,000 MW is far below even the worst-case projected demand of roughly 13,000 MW. This widening gap underscores the urgent need for sustainable and scalable alternative energy solutions. The 760 MW Kainji Hydropower Plant is one of Nigeria's most important hydro assets; however, it rarely operates at its full rated capacity due to hydrological constraints and aging units. Simultaneously, Nigeria boasts excellent solar energy resources, with average daily solar irradiation between 4.2 and 6.4 kWh/m²/day, especially in the northern region [4]. This creates strong opportunities for large-scale solar photovoltaic deployment.

Conventional ground-mounted solar PV systems face major challenges, including land-use conflicts, high installation costs, and environmental concerns. Floating Solar Photovoltaic (FSPV) systems offer an innovative and sustainable alternative by utilizing the surfaces of existing water bodies such as reservoirs, lakes, and hydropower dams for solar PV installation. By placing photovoltaic arrays on floating structures, FSPV eliminates competition for land while benefiting from water's natural cooling effect, thereby enhancing module efficiency, reducing thermal losses, and boosting annual energy output. Additional advantages include decreased water evaporation, inhibition of algal growth, and improved reservoir management [5].

A pioneering example of hybrid solar–hydropower systems integration is the Alto Rabagão Dam project in Portugal, developed by Energias de Portugal (EDP). Officially commissioned on July 6, 2017. The project marked a significant milestone in renewable energy development. It combines a 220 kWp floating solar PV system with a 68 MW hydroelectric power plant. The pilot installation features 2,500 squaAware4re meters of floating solar panels, which have the capacity to generate over 300 megawatt-hours annually [6]. Figure 2 shows the first floating solar PV Montalegre, Alto Rabagão dam, Portugal [3].

Figure 2: World's first hybrid hydro and floating solar plant at Alto Rabagao [3]

The Kainji Reservoir is exceptionally well-suited for such integration because of its large water surface area, existing 330 kV transmission infrastructure, strategic position within Nigeria's power network, and favourable solar irradiation levels. Integrating a utility-scale floating solar PV plant with the existing hydropower system offers a practical route to improving electricity reliability, increasing renewable energy penetration, and supporting Nigeria's transition to a low-carbon energy future [4].

This study focuses on the design and simulation of a 200 MWp Floating Solar Photovoltaic plant integrated with the 760 MW Kainji Hydropower Plant to evaluate its technical feasibility, structural viability, operational performance, and contribution to national grid stability.

1.1 Aim and Objectives

The main aim of this study was to design and simulate a 200 MWp floating solar photovoltaic power plant integrated with the 760 MW Kainji Hydropower Plant.

The specific objectives are:

i. To develop a design and simulation model for a 200 MWp FSPV system using PVsyst.
ii. To model floating platforms, anchors, and mooring systems using Google SketchUp.
iii. To evaluate the technical performance and operational synergy of the hybrid solar–hydropower system.

1.2 Study Area and Data Collection

The Kainji Reservoir, selected as the study location, lies in Niger State, Nigeria, at approximately latitude 10.39°N and longitude 4.61°E [7]. The reservoir covers about 1,270 km², has an average water depth of 12–15 m, and experiences seasonal water-level fluctuations of about ±4 m [2]. Global Horizontal Irradiance (GHI)

Received: 17/05/2026; Revised: 23/05/2026; Accepted: 02/06/2026; Published: 27/06/2026

averages 5.58 kWh/m²/day, and the annual solar resource exceeds 2,050 kWh/m²/year. The climate is tropical savannah with distinct wet and dry seasons [6]. The presence of existing 330 kV transmission lines significantly reduces additional evacuation infrastructure requirements, thereby improving the economic feasibility of hybrid solar–hydropower integration. These characteristics make the site highly suitable for large-scale floating solar photovoltaic deployment. Figure 3 presents the geographical location of the Kainji Reservoir as obtained from Google Earth [8].

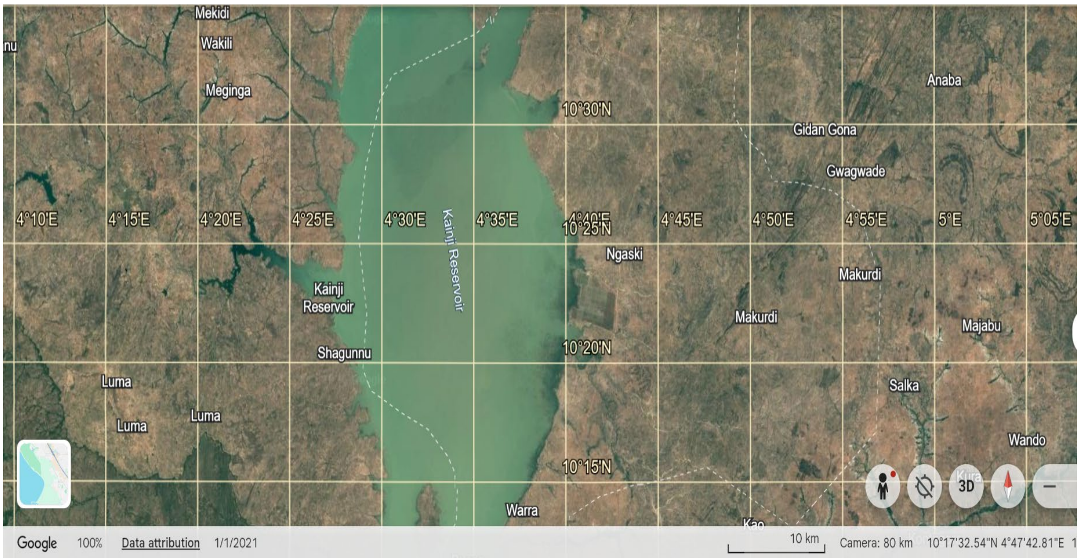

Figure 3: Kainji Reservoir map [8]

The major site characteristics used for system design and simulation are presented in Table 1.

Table 1: Site Characteristics of Kainji Dam

SN	Parameter	Value	Source
1	Coordinates	10.39°N, 4.61°E	Global Solar Atlas (2026)
2	Average. Depth	12–15 meters	NIWA Bathymetry (2023)
3	Water-Level Fluctuation	±4 m (seasonal)	Mainstream Energy Solutions Limited (MESL)
4	Approximate surface area of the reservoir	1,270 km²	HYPPADEC, FMWR
5	Total storage capacity	15 billion m³	FMWR
6	Wind Speed	108 km/h (30m/s)	Nigerian Meteorological Agency (NiMET)
7	Solar Irradiance	5.5–6.0 kWh/m²/day	NASA
8	Reservoir Surface Area	1,270,000,000 m²	HYPPADEC
9	Gross storage capacity	15 billion m³	HYPPADEC
10	Length of the reservoir	≈ 136 km	HYPPADEC
11	Maximum width of the reservoir	~ 24 km	HYPPADEC
12	Climate	Tropical savannah with distinct wet and dry seasons	NASA

2.0 Materials and Methods/Methodology

A quantitative engineering design and simulation approach was employed. The methodology comprised:

i. Solar resource assessment using NASA POWER, Global Solar Atlas, and Meteonorm data.
ii. PV system sizing using PVsyst simulation and mathematical validation.
iii. Floating platform design using High-Density Polyethylene pontoons based on buoyancy calculations.
iv. Structural modelling, anchoring, and mooring system design using Google SketchUp.
v. Hybrid system performance evaluation using PVsyst.

Hardware: A Dell laptop with Intel Core i7 processor, 32 GB RAM, and Windows 11.
Software: PVsyst (version 7.4), Google SketchUp (2024), and Microsoft Excel.

2.1 Floating Solar PV System Design and Simulation

This involves determining the optimal size of system components to connect the floating solar PV system with the hydropower plant. The plant's overall size and capacity depend on the water's surface area or the available

Received: 17/05/2026; Revised: 23/05/2026; Accepted: 02/06/2026; Published: 27/06/2026

space within the water body [9]. The floating solar PV system is similar in design to a conventional ground-mounted solar PV system, except that it requires a specific configuration to float on the water's surface [10]. A standard floating framework is employed to support the PV system. Solar PV arrays, inverters, combiner boxes, lightning arresters, and other components were housed. A mathematical method and PVsyst simulation were used in sizing system components based on meteorological and geographical system data.

2.1.1 Sizing PV Array

A 200 MWp system was designed using 600 W JINKO monocrystalline modules. The total number of modules required was computed as captured in Equation 1.

$$N_{PV} = \frac{P_{\text{plant}}}{P_{\text{module}}} = \frac{200{,}000{,}000}{600} = 333{,}334 \text{ modules} \quad (1)$$

For practical configuration, the value in equation 1 was rounded to 333,340 modules, consistent with PVsyst output. The optimal tilt angle for the site latitude of 9.87°N was determined using the rule-of-thumb formula:

$$\theta_{\text{tilt}} = \text{Latitude} \times 0.87 + 3.1 = 11.68^\circ \approx 12^\circ \quad (2)$$

Equation 2 was used to calculate the tilt angle using the rule-of-thumb formula. The panels face south with an azimuth angle of 0°. A fixed tilt was chosen over a tracking system to reduce wind loads and avoid mechanical complexity on water. The solar panel orientation of the 200 MWp plant, as extracted from PVsyst [11] are shown in Figures 4 and 5.

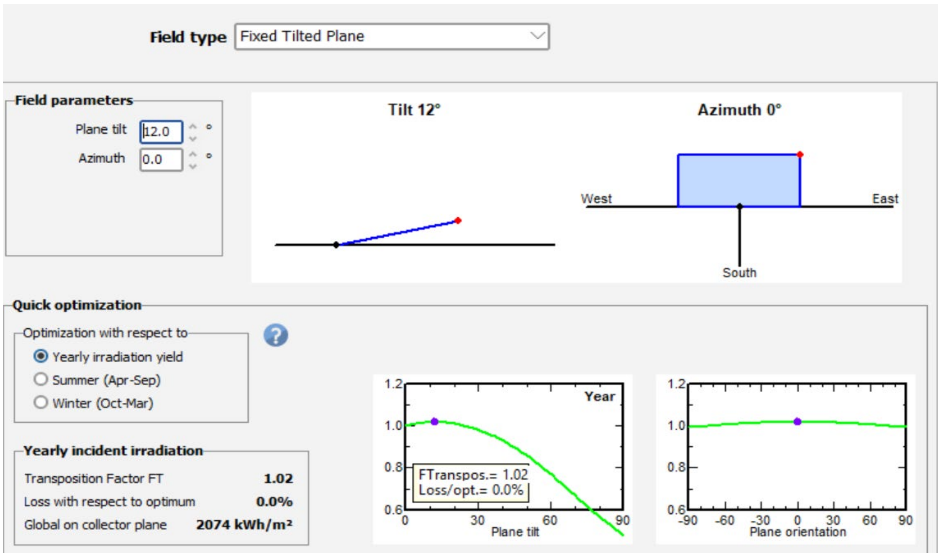

Figure 4: Solar Panel Orientation [11]

The solar PV field layout that presents the arrangement of PV modules on the Kainji Reservoir to generate the proposed 200 MWp is shown in Figure 5.

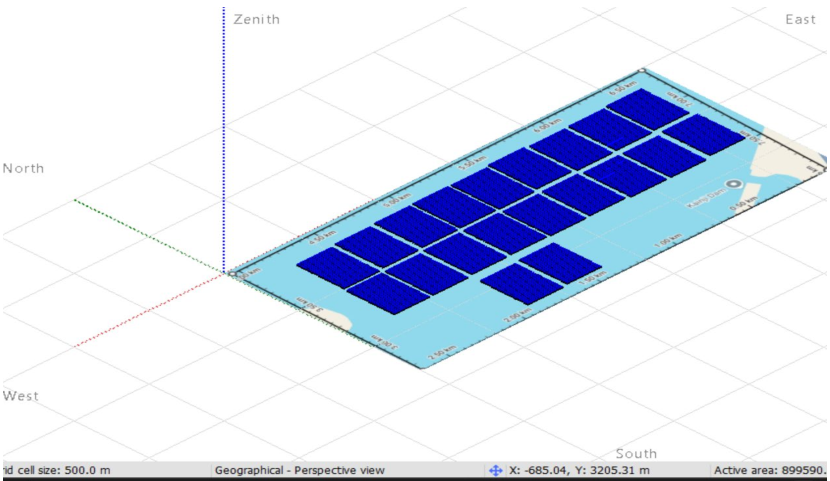

Figure 5: Solar PV field layout (Source: PVsyst)

The Solar field layout parameters are tabulated in Table 2.

Table 2: Solar Field Layout Parameters

SN	DESCRIPTION	VALUE
1	Module Capacity	600 W
2	Modules per substructure	200 units
3	Substructures per row	320 (long)/14.4 (short)
4	Rows per subfield	260 (long)1 (short)
5	Subfields (inverters)	619 units
6	Modules per row	780 (long)/432 (short)
7	Total modules	333,334 modules
8	Required area for the Modules	899,658 m²

2.1.2 Inverter Sizing

An inverter is a device that supplies AC loads by converting the DC output of the solar modules. Inverter's size can match the system's peak power, but it should have a 20 to 30 % tolerance to manage the initial surge current in the event of motor or compressor loads [12], [13]. It can be chosen according to the manufacturer's available capacity.

The DC/AC ratio (Inverter Loading Ratio, ILR) was set at 1.29 for tropical operating conditions. The total AC power output is:

$$P_{AC} = \frac{P_{DC}}{ILR} = \frac{200}{1.29} \approx 155 \text{ MW} \quad (3)$$

Equation 3 indicated that the AC output of inverters is 155 MW. Employing 250 kW Growatt grid-connected inverters (voltage range 500–1500 V, frequency 50 Hz):

$$N_{inv} = \frac{P_{AC}}{P_{inv}} = \frac{155{,}000}{250} = 620 \text{ inverters (619 in PVsyst due to rounding)} \quad (4)$$

Where, N_{inv} is the Number of inverters and P_{inv} is the Power of one inverter (kW). Equation 4 was used to calculate the total number of inverters in the system.

The power generated by a solar PV system is determined by the area of the PV panels, solar irradiance, and the efficiency of the PV modules, and the system efficiency can be determined by equation (5);

$$P = A_{PV} \times G \times \eta_{PV} \times \eta_{sys} \quad (5)$$

where P is the Output power (W), A_{PV} is the Total Area of the PV panels (m²), and G is the Solar irradiance (W/m²), which varies by location and time of day (typical peak value is around 1000 W/m²), η_{PV} is the PV panel efficiency (a typical range is 15-24 %, depending on the technology), and η_{sys} is the Overall system efficiency, which accounts for losses in inverters, cabling, and other components (usually around 80-90 %).

The arrangement of PV modules and inverters, based on the PVsyst simulation, is shown in Figure 6.

Received: 17/05/2026; Revised: 23/05/2026; Accepted: 02/06/2026; Published: 27/06/2026

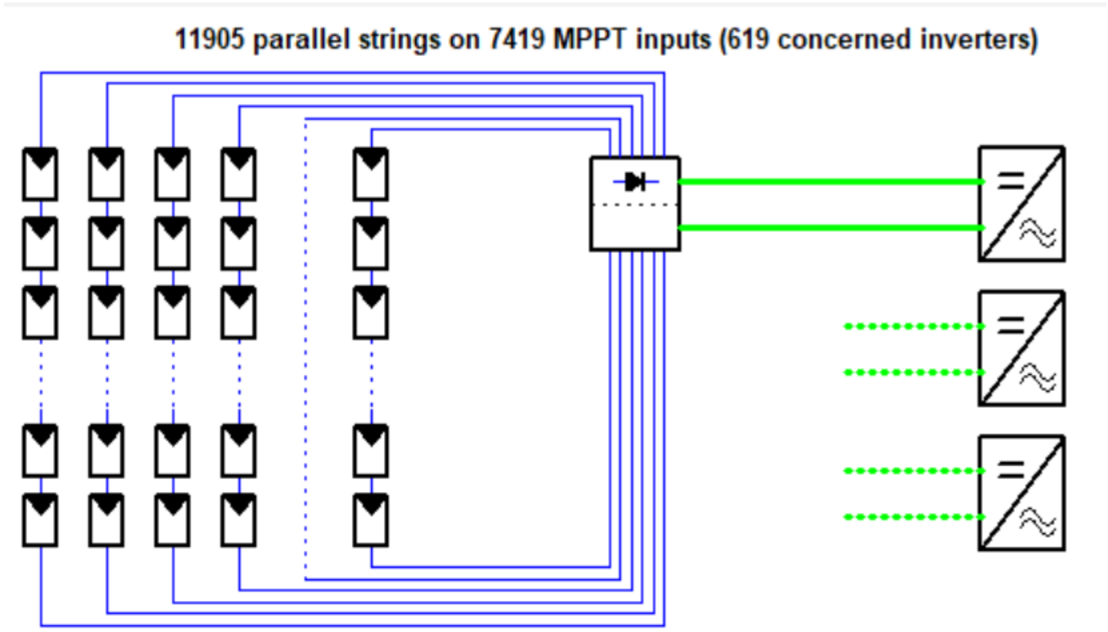

Figure 6: PV Modules and Inverters Arrangement (PVsyst)

2.1.3 Energy Yield Estimation

Using a simplified annual energy formula (for initial estimation):

$$E_{AC} = P_{DC} \times PSH \times 365 \times PR \quad (6)$$

$= 200{,}000 \times 5.58 \times 365 \times 0.7797 = 317{,}602{,}990$ kWh/year ≈ 317.6 GWh/year

The more accurate PVsyst hourly simulation, accounting for all real-world losses, yielded 322,129,399 kWh/year (322.1 GWh/year) at the P50 confidence level. The performance ratio (PR) was 77.97 % and the capacity factor (CF) is 18 %. The PVsyst simulation output is presented in Figure 7.

PV Array Characteristics

PV module		**Inverter**	
Manufacturer	Jinkosolar	Manufacturer	Growatt New Energy
Model	JKM-600N-66HL4M-BDV, degraded 2%	Model	MAX 250KTL3-X HV
(Custom parameters definition)		(Custom parameters definition)	
Unit Nom. Power	600 Wp	Unit Nom. Power	250 kWac
Number of PV modules	333340 units	Number of inverters	7419 * MPPT 8% 618.3 units
Nominal (STC)	200.0 MWp	Total power	154563 kWac
Modules	11905 string x 28 In series	Operating voltage	500-1500 V
At operating cond. (50°C)		Pnom ratio (DC:AC)	1.29
Pmpp	181.8 MWp	No power sharing between MPPTs	
U mpp	1037 V		
I mpp	175333 A		
Total PV power		**Total inverter power**	
Nominal (STC)	200004 kWp	Total power	154563 kWac
Total	333340 modules	Nb. of inverters	619 units
Module area	899658 m²		0.8 unused
		Pnom ratio	1.29
		Inverter PNom limit defined as apparent power	

Array losses

Thermal Loss factor		**DC wiring losses**		**Module Quality Loss**	
Module temperature according to irradiance		Global array res.	0.097 mΩ	Loss Fraction	-0.8 %
Uc (const)	29.0 W/m²K	Loss Fraction	1.5 % at STC		
Uv (wind)	0.0 W/m²K/m/s				
Module mismatch losses		**Strings Mismatch loss**		**Module average degradation**	
Loss Fraction	2.0 % at MPP	Loss Fraction	0.1 %	Year no	10
				Loss factor	0.4 %/year
				Mismatch due to degradation	
				Imp RMS dispersion	0.4 %/year
				Vmp RMS dispersion	0.4 %/year

Figure 5: PVsyst system simulation

Equation 7 shows the formula used in PVsyst to determine the energy to be produced.

Received: 17/05/2026; Revised: 23/05/2026; Accepted: 02/06/2026; Published: 27/06/2026

The annual AC energy output of a photovoltaic (PV) system is the total usable alternating current (AC) electricity delivered by the system over one year after accounting for system losses and conversion efficiency.

$$E_{AC} = \int_0^{8760} P_{AC}(t)\,dt = \int_0^{8760} \left[\frac{G_i(t)}{G_{STC}} \times P_{PV,rated} \times \eta_{PV}(T_c) \times \eta_{inv} \times \prod_{k=1}^{n}(1 - L_k)\right] dt \quad (7)$$

Where E_{AC} = Annual AC energy output (kWh/year), $P_{AC}(t)$ = Instantaneous AC power output at time t (kW), $G_i(t)$ = Instantaneous solar irradiance incident on PV module at time t (W/m²), G_{STC} = Solar irradiance at Standard Test Conditions = 1000 W/m², $P_{PV,rated}$ = Rated peak power of PV array at STC (kWp), $\eta_{PV}(T_c)$ = Temperature-dependent PV module efficiency (%), η_{inv} = Inverter efficiency (DC to AC conversion) (%), L_k = Individual loss factors (e.g., shading, soiling, wiring, mismatch), and n = Number of loss categories considered

PVsyst breaks down the calculation into a Loss Diagram with the following steps:

i. Initial Input (Global Horizontal Irradiance, (G_H): starts with hourly local meteorological data (GHI) for the Kainji location.
ii. Losses Before the Array (L_{before})
iii. PV Array Production (E_{Array}): This is the power produced by the panels before the inverter.
iv. System Losses (L_{system})
v. Final Output (E_{AC})

2.2 Structural modeling of floating platforms and anchoring systems

The floating platform was one of the most critical components of FSPV systems because it determines structural stability, buoyancy, maintenance accessibility, and long-term durability. Floating platforms provide mechanical support for PV modules and auxiliary equipment. These platforms are typically modular, allowing scalable deployment and flexible configuration. High-Density Polyethylene (HDPE) is widely used due to its corrosion resistance, UV stability, buoyancy, and low maintenance requirements [14].

2.2.1 Floating Structure and Buoyancy Requirements

The system utilized a modular pontoon structure to provide buoyancy and stability. High-Density Polyethylene (HDPE) pontoons were selected for their corrosion resistance, UV stability, buoyancy, and low maintenance requirements. Each 600 W module is supported by 12 pontoons, based on buoyancy analysis and manufacturer recommendations. Total number of pontoons:

$$N_{pontoons} = 333{,}340 \times 12 = 4{,}000{,}080\ pontoons \quad (8)$$

Relative to the plant capacity, the pontoon density is 20,000.4 pontons per MWp. The SketchUp design of a floating pontoon is shown in Figure 8**.**

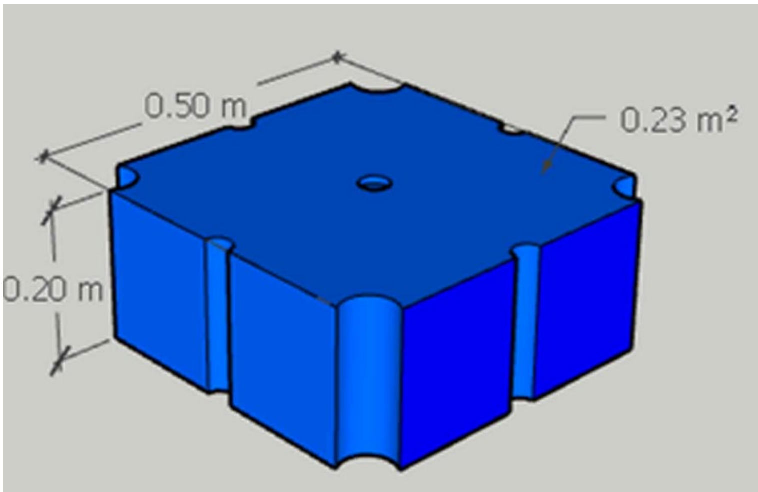

Figure 8: SketchUp Design of a Floating Pontoon Section

The buoyancy force followed Archimedes' principle as shown in equation 9.

$$F_b = \rho_{water} \times g \times V_{displaced} \quad (9)$$

The floating platform must displace a sufficient volume of water to counterbalance the weight of the platform and the PV equipment. The total deadload of a floating PV system typically consists of the following, as illustrated in Table 3.

Table 3: System Weight

SN	Item	Quantity	Weight per Unit (kg)	Total Weight (kg)
1	PV Modules	333,340 modules	30.5	10,166,870
2	Floating Platform structure (Floats/Pontoon)	Assumed 50% of PV Weight	-	5,083,435
3	Walkways & Maintenance	Assumed 10% of PV Weight	-	1,016,687
4	Electrical equipment (inverters, cables, etc)	Assumed 13% of PV Weight	-	1,333,008
5	**Total Weight**			**17,600,000 kg**
6	**Total Force**	Assumed acceleration due to gravity as 9.8m/s	**-**	**17.2x10^{8}N**

The volume of water displaced can be calculated using equation 10.

$$V = \frac{\text{Total Weight}}{\rho} \quad (10)$$

2.2.2 Reservoir Area and Floating Solar Potential

The Kainji Reservoir, with a total surface area of 1,270 km², has significant potential for floating solar PV development. To ensure the preservation of ecological zones and maintain navigation routes, it is standard practice to restrict floating photovoltaic (FPV) deployment to a small fraction of the total surface area. For this study, a conservative utilization factor of 3% is assumed, representing the practical feasible area. The available area for FPV deployment (A_{avail}) is calculated using equation 11.

$$A_{avail} = A_{total} \times f_{utilize} \quad (11)$$

Therefore, $A_{avail} = 38{,}100{,}000\ (or\ 3{,}810\ hectares)$

Based on industry benchmarks for power density, this feasible area could theoretically host up to 9 GWp of capacity. Consequently, the proposed 200 MWp plant is well within the ecological and operational limits of the reservoir.

2.2.3 Required Area for the Proposed 200 MWp System

The Kainji Reservoir Surface Area is 1,270,000,000 m²; the total practical area for floating PV is assumed to be 2–4% of the reservoir. Assuming 3%, the available area for floating solar is:

$$1{,}270\ kM^2 \times 0.03 = 38.1\ kM^2 = 38{,}000{,}000\ m^2$$

The total number of modules required for the floating area can be calculated using equation 12.

$$T_{modules} = \frac{A_F}{A_M} \quad (12)$$

Where,

$T_{modules}$ is the Total Modules, A_F is the Available area for Floating Solar PV and A_M is the Area of a Module (600W Jinko)

$$T_{modules} = \frac{38{,}000{,}000\ m2}{2.53\ m2\ per\ module} = 15{,}019762.85\ modules$$

By using 600 W per module, Kainji Reservoir can host up to 9 GW of floating PV without interfering with navigation or ecological zones. i.e $600\ W \times 15{,}415{,}019.8\ modules = 9{,}011{,}857{,}707.51\ W = 9\ GW$

The total water surface area required for the 200 MWp plant (A_{req}) is determined by the dimensions of the PV modules and the spacing required for the floating platform structure. According to the PVsyst design parameters, the plant requires 333,340 modules and occupies an estimated area of 899,658 m2. To account for inter-row spacing, maintenance walkways, and the floating structure, an area multiplier of 1.2 is applied to the footprint as shown in equation 13.

$$A_{req} = A_{mod} \times 1.2 \quad (13)$$

Where; A_{req}= Required area, and A_{mod} = Surface area of module = 899,658 m²

$= 899{,}658\ \text{m2 x } 1.2 = 1{,}079{,}589.60\ \text{m2}$ (approximately 108 hectares)

The proposed 200 MWp capacity utilizes only 2.84 % of the total feasible floating area (38.1 million m²), demonstrating significant potential for future expansion. It is important to prioritize areas away from hydro intakes, spillways, and navigation channels to avoid possible shading.

2.2.4 Anchoring and Mooring

For a 200 MWp floating solar PV (FPV) system on the Kainji Reservoir, the anchoring and mooring system is a critical engineering component. The system must account for the high drag forces generated by the large surface area of the FPV array and the significant seasonal water level fluctuations characteristic of the Kainji Reservoir.

2.2.4.1 Anchor Sizing

The following parameters and assumptions serve as the basis for the structural calculations of the anchor and mooring points.

Table 4: Assumptions in Sizing an Anchor

SN	Parameter	Typical Value
1	Anchor use	Floating PV platform (HDPE + PV)
2	Water Depth	~10-20 m
3	Maximum Wind Speed (design basis)	108 km/h (~30 m/s)
4	Platform load per Anchor point	~10-30 kN
5	Friction Coefficient (concrete/mud)	~0.5-0.6
6	Safety Factor	1.5-2.0

Designing concrete deadweight anchors for a floating solar PV system on Kainji Reservoir requires calculating their size based on buoyancy, wind, wave forces, and depth.

2.2.5 Force Estimation and Anchor Mass Calculation

The required resisting force of the concrete dead weight must overcome the horizontal sliding force exerted by wind and wave action. The required submerged weight of the anchor (F_R) is calculated using the following relationship by assuming an average horizontal load per mooring of 25–30 kN as shown in equation 14.

$$F_{resist} = \frac{F_H \times SF}{\mu} \qquad (14)$$

Where,
F_{resist} is the Force Estimation per Anchor
F_H is the Average Horizontal Load per Mooring
SF is the Safety Factor
μ is the Friction Coefficient

The recommended anchor dimensions per block are tabulated in Table 5.

Table 5: Anchor Dimensions

S/N	Shape	Dimension (LxWxH)	Volume (M³)	Weight (kg)
1	Cubic	1.7 m × 1.7 m × 1.7 m	4.91 m³	~11,800 kg
2	Rectangular	2.0 m x 2.0 m x 1.25 m	5.0 m³	~12,000 kg
3	Trapezoidal	2.2 top/2.8base x 2.2 x 1.2	~5.1 m³	~12,200 kg

A rectangular shape anchor was used in this research, as shown in Figure 9, based on the SketchUp design.

Received: 17/05/2026; Revised: 23/05/2026; Accepted: 02/06/2026; Published: 27/06/2026

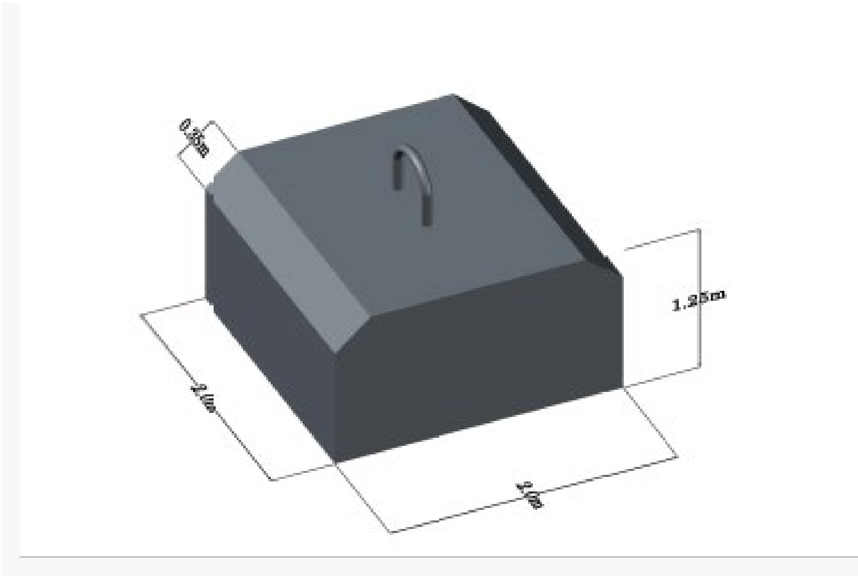

Figure 9: Concrete Block- Sketchup Design

According to the Zimmerman Floating PV system website, 1 to 3 anchors are required per MWp for large-scale floating solar projects [15]. Therefore, using three anchors per MW, the total number of anchors for this research is 600.

2.2.6 Wind Force on Floating Structure

Wind force is caused by the pressure exerted by moving air on exposed structural surfaces. Unlike waves and currents (which act mainly underwater), wind predominantly affects the freeboard, superstructure, and equipment above the water line. Wind loading is highly variable and depends on wind speed, direction, gusts, and turbulence.

The wind force acting on a floating structure is generally calculated using Equation 15.

$$F_{wind} = 0.5 \times C_d \times \rho_{\text{air}} \times A \times V^2 \quad = 836{,}797{,}500 \text{ N} \tag{15}$$

where F_{wind} is the Wind force in Newtons (N), ρ is the Air density (≈ 1.265 kg/m³), A is the Total surface area exposed to wind (≈ 1,226,333 m²), C_d is the Drag coefficient (≈ 1.2 for flat surfaces), and V is the Wind speed (≈ 30 m/s)
To ensure safety under extreme conditions, a safety factor can be applied as shown in equation 16.

$$F_{anchor} = F_{wind} \times SafetyFactor \tag{16}$$

Applying a safety factor of 1.5, F_{wind} is the estimated wind force given as 836,797,500 N, and F_{anchor} is the Anchor Load. Assuming 600 anchors equally sharing the load, the load per anchor can be determined as illustrated in Equation 17.

$$\text{Load per anchor} = \frac{F_{anchor}}{600} \tag{17}$$

2.2.7 Water Current Force, F_c

Assuming a water current velocity of 1 m/s, and a drag coefficient of 1.0, Equation 18 can be used to calculate the water current force.

$$F_c = 0.5 \times C_d \times \rho_{\text{water}} \times A_{\text{submerged}} \times V_c^2 \tag{18}$$

2.2.8 Total Mooring Force

The total mooring force ($F_{mooring}$) is the sum of all the forces acting on the floating PV system (wind, wave, and current forces). For stability, the mooring system should be designed to counteract the combined force using Equation 19.

$$F_{mooring} = F_w + F + F_{current} \tag{19}$$

Received: 17/05/2026; Revised: 23/05/2026; Accepted: 02/06/2026; Published: 27/06/2026

2.2.9 Mooring Line Tension and Elasticity

The mooring lines experience tension due to the forces acting on the platform. To avoid failure, the maximum tension Tmax in each line must be below the breaking strength of the line as shown in Equation 20.

$$T_{max} = \frac{F_{mooring}}{N \times cos\theta} \quad (20)$$

where T_{max} is the Maximum tension in each mooring line (N), N is the Number of mooring lines, θ is the Angle between the mooring line and the seabed (typically 30°–60°).

For flexible mooring lines, elasticity can absorb some force and help maintain tension. Hooke's law calculates the elastic elongation ΔL as illustrated in Equation 21.

$$\Delta L = \frac{T}{EA} \quad (21)$$

where, ΔL is the Elongation of the mooring line (m), T is the Tension in the mooring line (N), E is the Elastic modulus of the mooring line material (Pa), and A is the Cross-sectional area of the mooring line (m²).

2.2.10 Mooring Line Length

Assuming a 45° angle and a water depth of 15 m

$$L = \frac{D}{sin\theta} = \frac{15}{sin45} = 21.21\ meter$$

Where,
L is the Mooring line length, D is the Depth of the reservoir (15 meters), and θ is the Angle of the mooring line (45°). This length ensures that the mooring system can accommodate water-level fluctuations and maintain tension without overstressing the anchors.

2.3 System Performance and Hybrid Operation

The system performance was evaluated using the annual energy yield, performance ratio (PR), capacity factor (CF), specific yield, system losses, grid contribution, and solar–hydro complementarity.

2.3.1 Performance Metrics

i. Performance Ratio (PR) = $\frac{E_{\text{actual}}}{E_{\text{theoretical}}} = 77.97\ \%$

ii. Capacity Factor (CF) = $\frac{322{,}129{,}399}{200{,}000 \times 8760} = 0.184 = 18.4\ \%$

iii. Specific yield = 1,610 kWh/kWp/year

The benchmark against existing tropical FSPV projects is tabulated in Table 6:

Table 6: Benchmark Against Tropical FSPV Projects

SN	Project	Location	Year	Capacity	PR	CF
1	Omkareshwar	India	2023	90 MWp	78.50%	17.90%
2	Tengeh Reservoir	Singapore	2021	60 MWp	78.29%	18.10%
3	Sirindhorn Dam	Thailand	2021	45 MWp	77.50%	17.8%
4	This Study (Kainji)	Nigeria	-	200 MWp	77.97	18.00%

The results are consistent with leading FSPV installations worldwide.

2.3.2 Uncertainty Analysis and Energy Yield Probability Assessment

Since weather data varies from year to year, the probability of getting a particular output from the plant has to be determined considering the year-to-year variability. Uncertainty analysis quantifies the confidence level associated with the simulated annual energy production. PVsyst typically report energy yields at P50, P75, and P90 confidence levels. According to this research simulation, the annual energy production probabilities at Year-to-year variability of 5.1 % are:

i. P50 (50% probability of exceedance): 322.1 GWh/year
ii. P90 (90% probability): 300.5 GWh/year
iii. P95 (95% probability): 294.4 GWh/year

Received: 17/05/2026; Revised: 23/05/2026; Accepted: 02/06/2026; Published: 27/06/2026

2.4 Hybrid solar–hydropower operational modeling

The hybrid model allows solar PV generation during daytime periods while hydropower conserves water for evening peak demand and dry-season support. This operational strategy improves dispatch flexibility, reservoir management, generation reliability, and grid stability. Hydropower acts as a virtual energy storage system, thereby reducing the need for battery energy storage systems. Hybrid operation was modeled using a simplified dispatch relationship:

$$P_{grid}(t) = P_{PV}(t) + P_{Hydro}(t) \tag{22}$$

Daytime water conservation constraint:

$$P_{Hydro}(t) = P_{load}(t) - P_{PV}(t) \tag{23}$$

Key benefits observed include:

i. Improved load-following capability
ii. Reduced intermittency of solar generation
iii. Enhanced grid stability and frequency regulation

The existing 330kV transmission infrastructure was used for grid evacuation, significantly reducing additional infrastructure costs. The grid interconnection of the hybrid system is to be shared via an existing Kainji switchyard to the National grid through:

i. 330 kV Kainji-Jebba Double Circuit Transmission Line
ii. 330 kV Kainji-Birnin Kebbi Double Circuit Transmission Line
iii. 330 kV Kainji-Fakun Double Circuit Transmission Line

The Single Line Diagram (SLD) of the Hybrid system is shown in Figure 10.

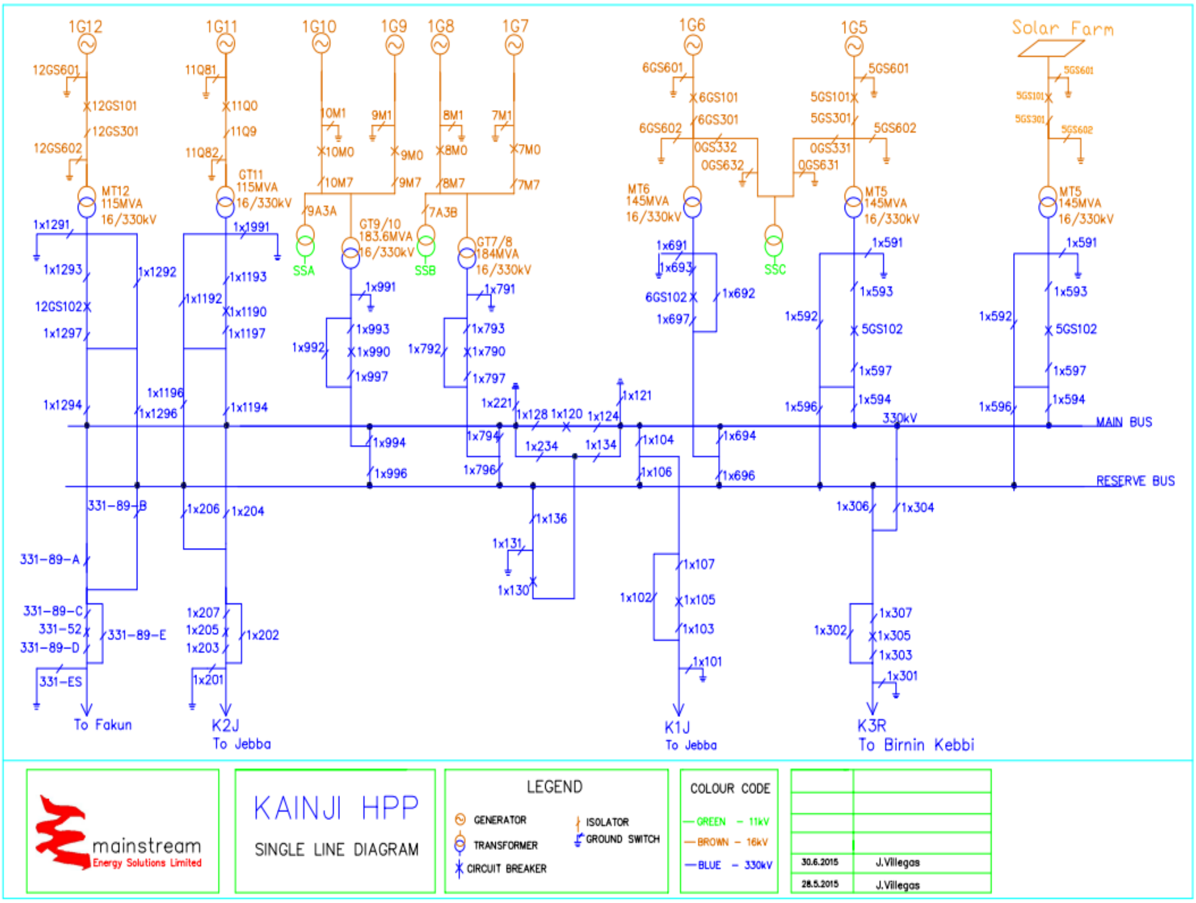

Figure 10: Single Line Diagram for the Hybrid System

3.0 Results and Discussions

This chapter presented and discussed the results obtained from the design, simulation, and performance evaluation of the 200 MWp Floating Solar Photovoltaic (FSPV) system integrated with the 760 MW Kainji

Hydropower Plant. Emphasis is placed on interpreting the findings in relation to grid stability, efficiency improvements, and practical implementation at the Kainji Reservoir.

The meteorological and geographical system data results were used in sizing system components. The monthly and hourly solar irradiance results are shown in Figures 11 and 12, respectively.

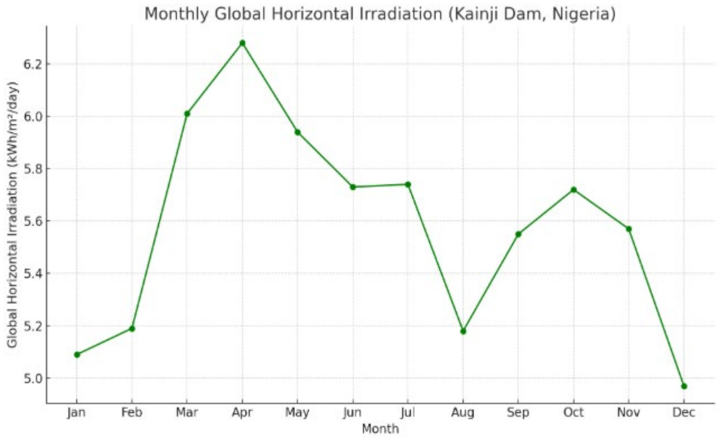

Figure 11: Monthly Global Horizontal Irradiation of Kainji Dam (Source: PVsyst)

Figure 11 shows the monthly global horizontal irradiance curve of the Kainji Dam location, which is one of the critical components considered in site selection and system sizing for optimal generation output. The figure shows that the proposed plant may experience high generation output in April due to high irradiance and low output in December, January, and August due to low irradiance. Figure 12 shows the hourly irradiance as extracted from the Global Solar Atlas.

	Jan	Feb	Mar	Apr	May	Jun	Jul	Aug	Sep	Oct	Nov	Dec
0 - 1												
1 - 2												
2 - 3												
3 - 4												
4 - 5												
5 - 6				0.156	0.490	0.731	0.470	0.412	0.548	0.446	0.051	
6 - 7	3.596	3.838	5.302	12.038	14.440	13.932	12.238	11.959	14.528	17.786	17.043	6.668
7 - 8	31.784	30.150	32.909	38.803	39.331	36.255	33.515	32.636	39.199	48.342	52.318	43.243
8 - 9	64.255	62.515	64.210	68.081	65.500	59.620	53.814	51.682	64.290	76.795	85.051	76.943
9 - 10	93.141	91.418	92.450	93.033	88.089	79.157	69.792	67.321	83.597	99.893	111.145	103.804
10 - 11	112.708	112.488	112.015	110.138	103.531	92.822	83.250	80.831	101.380	117.417	127.856	120.972
11 - 12	121.672	122.956	120.907	116.303	108.264	100.180	91.640	90.011	112.147	125.790	132.516	127.227
12 - 13	118.969	121.652	118.673	113.131	108.050	99.178	92.134	90.781	110.148	120.762	125.551	122.333
13 - 14	105.314	108.346	104.096	99.470	95.142	89.906	84.960	82.674	95.721	104.314	107.599	106.591
14 - 15	81.771	84.718	80.198	77.160	74.875	72.989	71.264	67.888	75.067	79.057	81.276	81.472
15 - 16	51.536	55.114	51.445	49.556	49.989	50.366	51.396	49.284	50.988	48.328	47.856	49.391
16 - 17	18.578	24.058	22.434	21.632	23.219	25.048	26.840	25.181	21.579	15.376	13.934	15.666
17 - 18	0.251	1.950	2.028	1.891	2.528	3.896	4.681	4.251	1.234	0.049		0.049
18 - 19												
19 - 20												
20 - 21												
21 - 22												
22 - 23												
23 - 24												
Sum	804	819	807	801	773	724	676	655	770	854	902	854

Source: globalsolaratlas.info

Figure 12: Hourly profile of solar irradiance (Global Solar Atlas, 2026)

Figure 12 shows that peak hourly irradiance is typically observed between 11:00 am and 2:00 pm during the months of January to April, and again from October to December, aligning well with Nigeria's daytime electricity demand profile n Table 17 and Figure 23, respectively. These characteristics confirmed that the site received consistently strong solar irradian throughout the year, hence the suitability of the Kainji Reservoir for the proposed 200 MWp floating Solar PV plant deployment. The resource consistency supports high specific yield and informed PV/inverter sizing in PVsyst.

3.1 PV System Sizing Results

A PVsyst simulation resulted in a system configuration comprising:

i. 333,340 monocrystalline PV modules rated at 600 W each, arranged in 11,905 strings with 28 modules connected in series per string to generate 200 MWp.

Received: 17/05/2026; Revised: 23/05/2026; Accepted: 02/06/2026; Published: 27/06/2026

ii. A tilt angle of 12° with south-facing orientation, ensuring optimal solar irradiance capture under the site-specific conditions.
iii. In terms of spatial requirements, the PV array occupies a reservoir surface area of approximately 899,658 m² (0.899 km²).
iv. A total occupied water surface area of approximately 1.01 km², including maintenance spacing, was established. This coverage represents only 2.7 % of the feasible floating area of the Kainji Reservoir, demonstrating that large-scale FPV deployment is achievable with minimal spatial impact.

The photovoltaic array consists of 333,334 modules installed at a fixed tilt angle of 12°. A fixed-tilt configuration was selected over a tracking system to limit wind-induced aerodynamic loads, thereby enhancing structural stability and reducing mechanical fatigue risks to the floating platform. The estimated annual energy yield of 322.1 GWh significantly contributes to Nigeria's grid stability and energy mix. Seasonal variation aligns well with hydropower generation, enabling effective hybrid dispatch. Figure 13 shows the PVsyst result on tilt-angle vs. the annual energy generation curve.

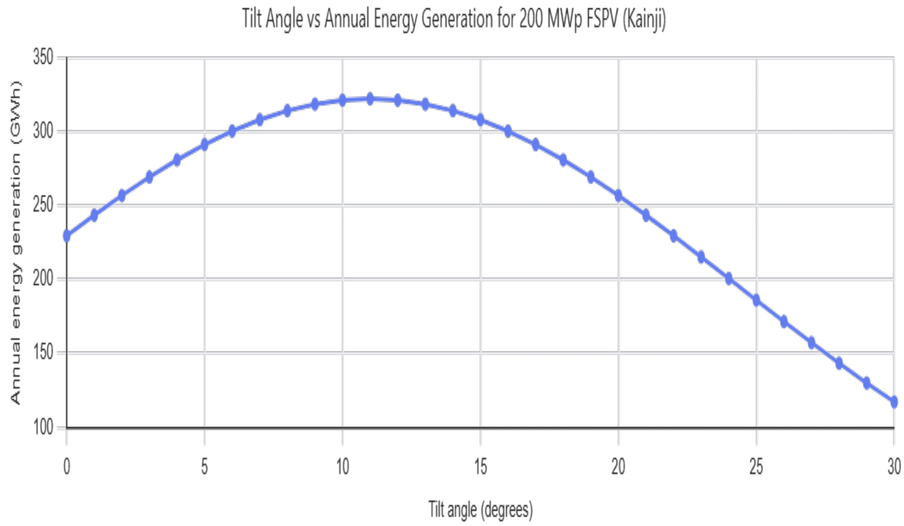

Figure 13: Tilt Angle vs Annual Energy Generation for 200 MWp FSPV (Kainji)

A fixed-tilt configuration of 12° was selected over a tracking system to limit wind-induced aerodynamic loads, thereby enhancing structural stability and reducing mechanical fatigue risks to the floating platform.

String inverters were deployed to improve system redundancy, facilitate fault isolation, and support ease of maintenance, contributing to long-term operational sustainability. The monthly generation output of the FSPV plant is shown in Figure 14.

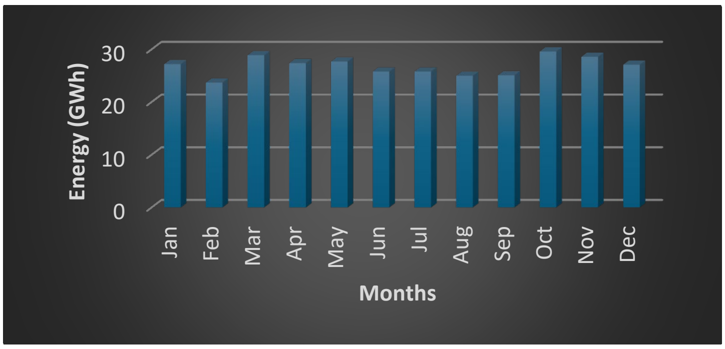

Figure 14: Monthly Energy Generation of FSPV Plant

The relatively high Annual Energy Production is attributed to:
i. High solar resource availability at the Kainji Dam site (GHI ≈ 2,050 kWh/m²/year),
ii. Reduced thermal losses due to the cooling effect of the water surface,
iii. Low soiling losses compared to land-based PV systems,
iv. Minimal shading results from the open-water installation.

3.2 Floating Solar PV Plant Performance Analysis

The simulation results indicate that the proposed FSPV system achieves an annual energy yield of approximately 322,129,399 kWh/year, with a performance ratio (PR) of 77.97 % and a capacity factor of 18 %.

	GlobHor	DiffHor	T_Amb	GlobInc	GlobEff	EArray	E_Grid	PR	EArrMPP
	kWh/m²	kWh/m²	°C	kWh/m²	kWh/m²	kWh	kWh	ratio	kWh
January	157.7	79.4	27.38	172.3	169.2	27588264	27248068	0.791	28370173
February	145.3	87.9	29.78	152.6	149.7	24050492	23744041	0.778	24884903
March	186.4	101.4	31.16	190.1	186.7	29289864	28928696	0.761	30821595
April	188.4	94.5	29.98	185.1	181.6	28814714	27438502	0.741	30169445
May	184.0	92.7	28.73	174.8	170.9	28091889	27742675	0.793	28671711
June	172.0	85.7	26.42	160.9	157.0	26166017	25842554	0.803	26592241
July	177.9	84.3	25.89	166.7	162.1	27007394	25804186	0.774	27553090
August	160.6	91.1	25.08	155.6	151.6	25309670	25001303	0.804	25856025
September	166.4	82.9	25.17	167.0	163.2	26520087	25097422	0.751	27669383
October	179.0	86.7	26.62	187.7	184.0	29903117	29554022	0.787	30980942
November	167.0	71.3	27.42	183.1	179.6	28957031	28617657	0.781	30059762
December	154.0	79.7	27.41	169.8	166.4	27434580	27110275	0.798	27949060
Year	2038.6	1037.6	27.57	2065.7	2022.1	329133119	322129399	0.780	339578328

Legends

GlobHor	Global horizontal irradiation	EArray	Effective energy at the output of the array
DiffHor	Horizontal diffuse irradiation	E_Grid	Energy injected into grid
T_Amb	Ambient Temperature	PR	Performance Ratio
GlobInc	Global incident in coll. plane	EArrMPP	Array virtual energy at MPP
GlobEff	Effective Global, corr. for IAM and shadings		

Figure 15: Plant Performance (Source: PVsyst)

The results indicate strong predictability and financial viability of the proposed floating solar system, confirming its bankability and consistency with high-performing floating solar installations in tropical regions. The performance ratio of 77.97 % is higher than that of conventional ground-mounted PV systems, which typically range between 70–75 %. This improved efficiency is mainly due to the cooling effect of the reservoir, which lowers module operating temperature, reduces dust accumulation, enhances solar irradiance absorption, and supports optimized system performance through PVsyst simulation.

System losses were assessed in terms of thermal losses, inverter conversion losses, cable (ohmic) losses, and mismatch losses. Thermal losses were significantly lower than in land-based systems because the water body acts as a natural heat sink, improving PV module efficiency at lower temperatures. Inverter and electrical losses remained within acceptable engineering limits, confirming proper system sizing and an appropriate DC/AC ratio. In addition, the high solar resource availability at Kainji Hydropower Plant contributes to the strong specific yield and capacity factor achieved. These findings demonstrate that floating solar PV systems offer enhanced technical performance and efficiency under the hot tropical climatic conditions of northern Nigeria.

Received: 17/05/2026; Revised: 23/05/2026; Accepted: 02/06/2026; Published: 27/06/2026

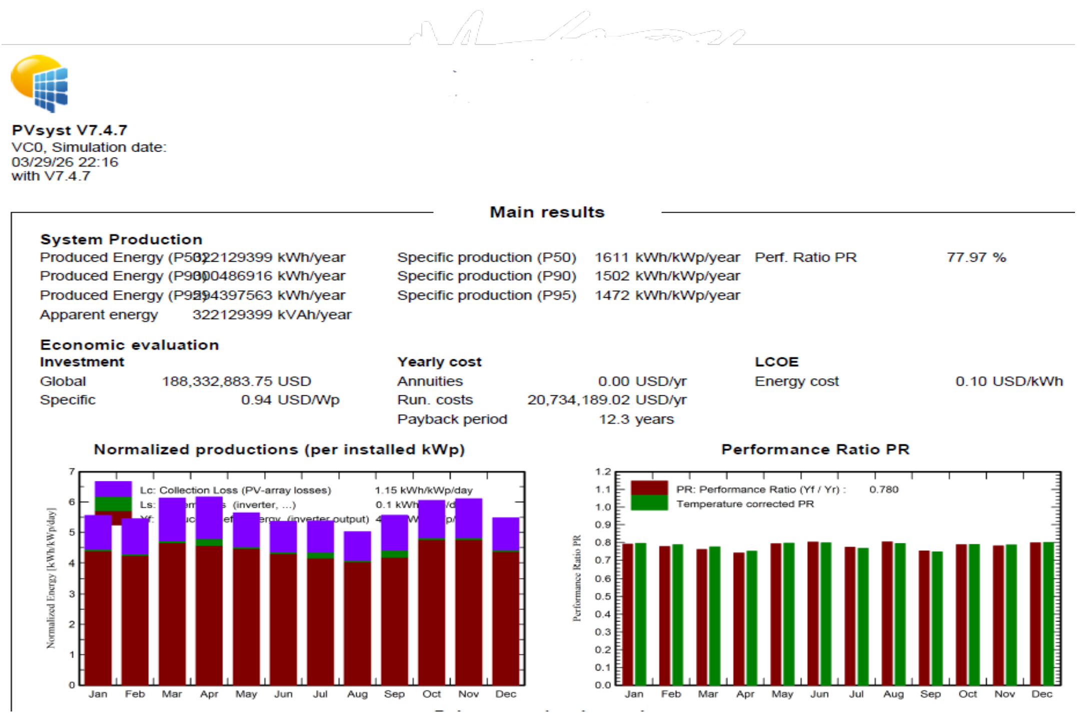

Figure 16: Plant Performance (source: PVsyst)

According to the results, the highest energy production per installed kWp is in April due to high solar irradiance.

3.2.1 P50, P90 and P95 Performances

Since weather data varies from year to year, the probability of getting a particular output from the plant has to be determined. Considering the year-to-year variability of 5.1 % and the global variability of 5.4 %, Figure 22 presents the P50, P90, and P95 plant performances. It will be seen that the P90 performance is 300.5 GWh/year, which means there is a 90 % probability that the plant will produce the amount every year.

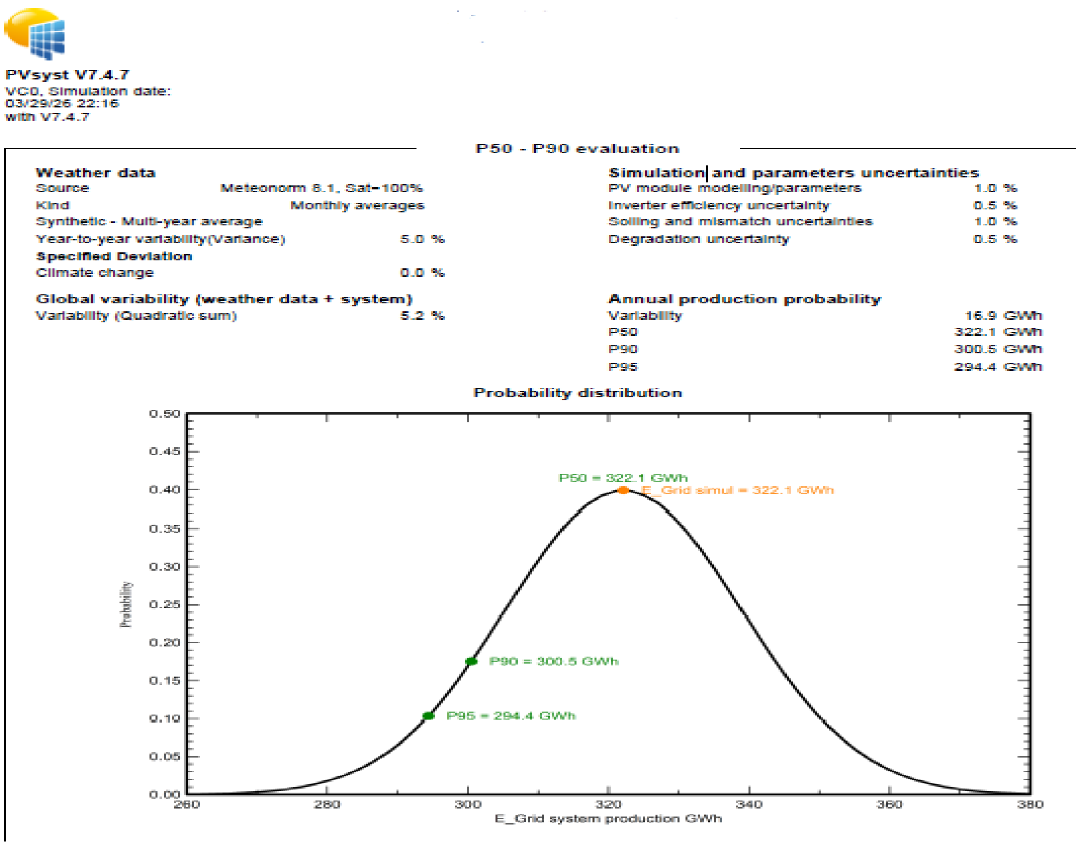

Figure 17: Probability Distribution against the annual system production curve

Received: 17/05/2026; Revised: 23/05/2026; Accepted: 02/06/2026; Published: 27/06/2026

The figure indicates that the P90 energy yield is 300.5 GWh/year, implying a 90 % likelihood that the plant will achieve at least this level of annual generation. Similarly, the P50 energy yield is estimated at 322.1 GWh/year, while the more conservative P95 estimate is 294.4 GWh/year.

3.3 Structural Feasibility of the Floating Platform

The buoyancy and structural analyses demonstrate that the proposed pontoon-based floating platform can safely support the 200 MWp installation with adequate safety margins. The modular design enhances scalability and ease of maintenance while minimizing structural complexity.

The result of the configuration revealed that 12 pontoons can be used per 600 W PV module and approximately 22,000 pontoons per MWp of installed capacity of 200 MWp. Notably, the result shows that the proposed 200 MWp system utilizes only about 2.7 % of the available feasible floating area of 38 km², indicating substantial potential for future expansion without significant spatial constraints. The buoyancy force of 258,720,000 N keeps the floating platform above water and is equal to the weight of the water displaced by the submerged portion of the platform. The buoyancy and structural design calculations confirm that the floating solar platform can support the 200 MWp system with adequate safety margins.

3.3.1 Anchor and Mooring Line Tension

A total of 600 rectangular-shaped deadweight anchors that consist of concrete blocks are considered due to the nature of the soft sediment of the Kainji dam, with an approximate 2,092 kN per anchor. An estimated wind force acting on a floating structure for the proposed research of 836,798 kN was caused by the pressure exerted by moving air on exposed structural surfaces. Wind predominantly affects the freeboard, superstructure, and equipment above water level. Wind loading is highly variable and depends on wind speed, direction, gusts, and turbulence. The anchor force of 1,255,196,250 N indicates that the system can withstand environmental stresses typical of the Kainji reservoir. The use of deadweight anchors is appropriate given the soft sediment bed conditions, ensuring both cost-effectiveness and structural reliability.

3.4 Hybrid Hydro–Solar System Performance

The 760 MW Kainji Hydropower Plant's generation output is based on the typical hydrology of the Niger River, seasonal inflow patterns (wet vs dry season), and historical operation trends (reduced output due to water levels and unit availability).

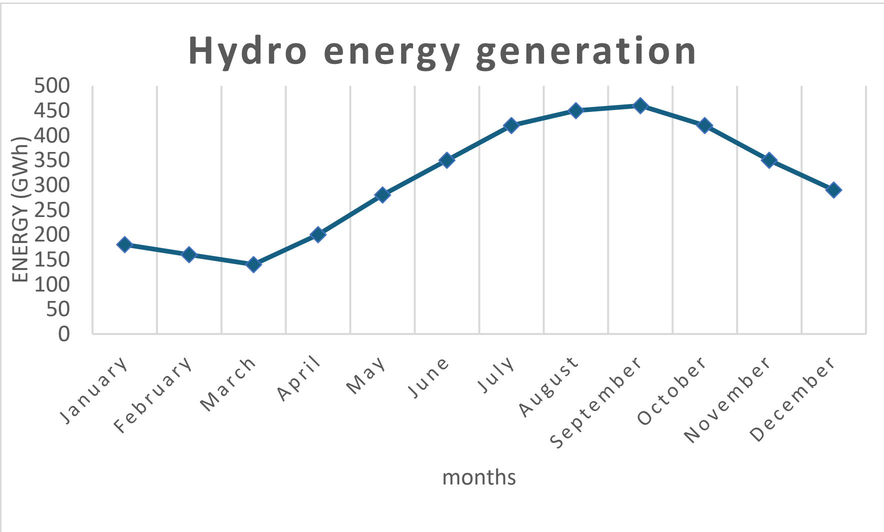

Figure 18: Monthly Energy Generation of Kainji Hydropower Plant

The results show that the Kainji Hydropower Plant operates strongly based on seasonal rainfall patterns and upstream river discharge. Peak electricity generation occurs in August and September, reaching about 450–460 GWh due to high water inflow, while the lowest generation is recorded in February and March at approximately 140–160 GWh because of reduced inflow.

The hybrid floating solar–hydropower configuration improves grid reliability by addressing both solar intermittency and seasonal hydropower fluctuations. Solar PV supplies daytime peak demand, while hydropower compensates during low solar generation periods, creating a strong complementary relationship. This allows hydropower to function as a virtual energy storage system, reducing dependence on expensive battery storage and

Received: 17/05/2026; Revised: 23/05/2026; Accepted: 02/06/2026; Published: 27/06/2026

improving dispatch flexibility. The highest combined hybrid energy output occurs between August and September at about 485.10 GWh, driven by peak hydropower inflows, while the lowest is recorded in March at approximately 168.93 GWh before the rainy season begins. With an annual combined generation of nearly 4 TWh, the hybrid system significantly smooths seasonal variability, enhances operational stability, and strengthens the reliability of Nigeria's power grid.

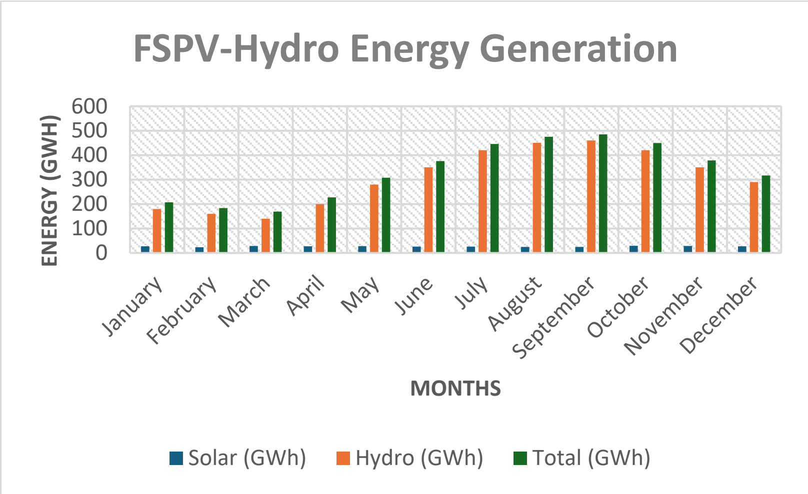

Figure 19: Hybrid Energy Generation Output of the System

The highest combined energy output is between August and September (≈485.10 GWh), driven by peak hydropower inflows, while the lowest is in March (≈168.93 GWh), before peak rainy-season inflows with an annual generation of approximately 4 TWh. The overall effect is that the hybrid system significantly smooths seasonal variability. A hybrid solar–hydropower dispatch strategy allows daytime solar production to meet demand while preserving reservoir water for nighttime operation and peak demand intervals. This operational synergy enhances system flexibility and mitigates reliance on hydropower generation during dry seasons.

This synergy is particularly important for Nigeria's grid, which suffers from instability and fluctuating generation capacity. The Single Line Diagram of the hybrid system is shown in Figure 20.

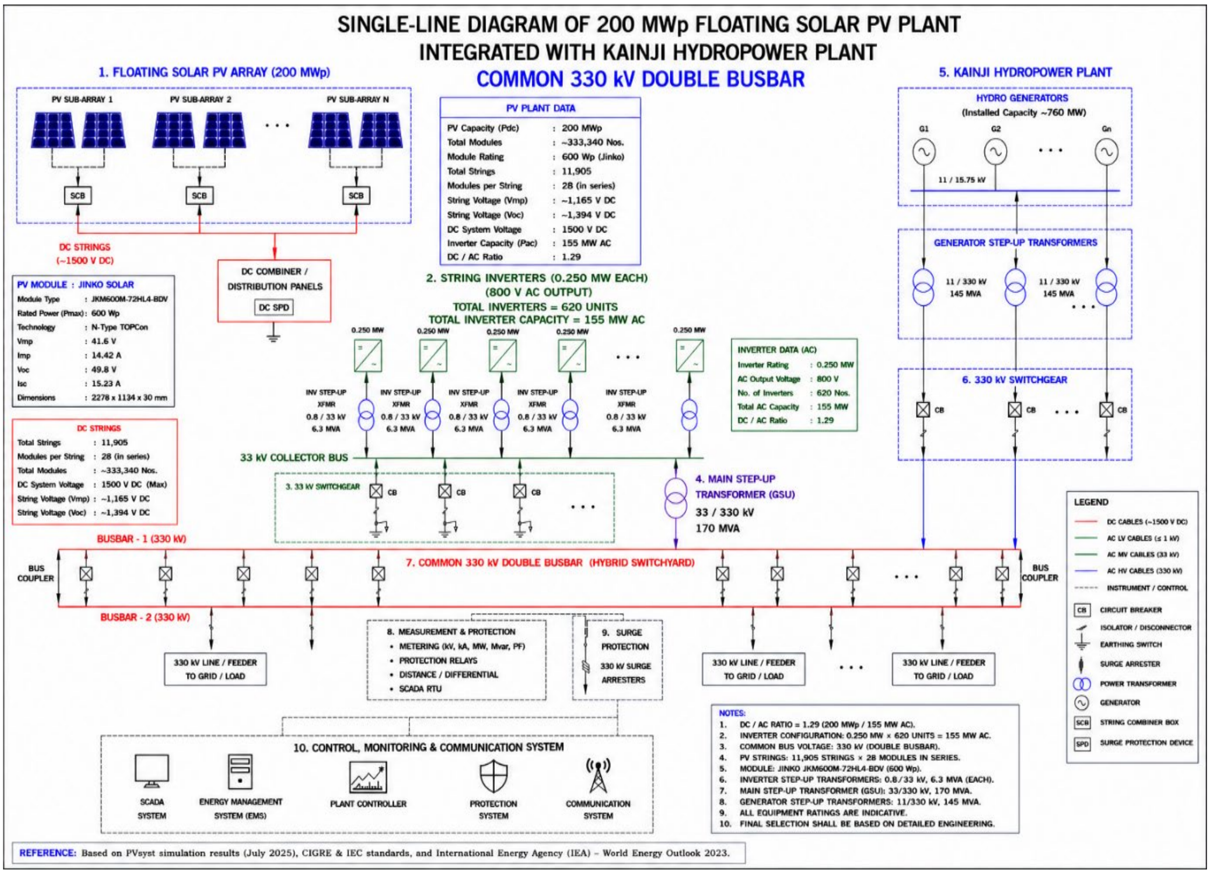

Figure 20: FSPV-Hydro Plant Hybrid Single Line Diagram

Received: 17/05/2026; Revised: 23/05/2026; Accepted: 02/06/2026; Published: 27/06/2026

The Figure illustrates the interconnection of a 200 MWp solar PV plant with 760 MW. The solar PV plant's a/c output power is connected to the common busbar with the eight (8) turbines of the hydropower plant, with ratings of 4x80 MW Kaplan turbines, 2x100 MW Kaplan turbines, and 2x120 MW propeller turbines. The combined inverters' A/C output of 155 kW, 33/330 kV was connected to a common 330 kV busbar through a 170 MVA step-up transformer.

4.0 Conclusion

This research developed and simulated a 200 MWp Floating Solar Photovoltaic (FSPV) system integrated with the 760 MW Kainji Hydropower Plant to address Nigeria's electricity supply challenges. The study focused on improving the use of existing hydropower infrastructure, reducing land requirements for solar installations, and utilizing Nigeria's abundant solar resources. The system was designed and evaluated based on meteorological, reservoir, and structural data, using analytical modeling and simulation tools such as PVsyst and Google SketchUp. The system requires 333,340 monocrystalline modules at a 12° tilt, using approximately 4.0 million HDPE pontoons. Results showed that the proposed FSPV system can generate about 322.1 GWh annually, with a performance ratio of 77.97 % and a capacity factor of 18 %, while occupying only 2.7 % of the reservoir's feasible surface area. The hybrid solar–hydropower configuration improves grid flexibility by allowing hydropower to serve as virtual energy storage. Overall, the study confirmed that integrating floating solar PV with Kainji Dam is a technically feasible and sustainable solution for enhancing Nigeria's renewable energy generation and grid stability. The annual combined generation reaches approximately 4 TWh (3.2 TWh from hydro plus 0.322 TWh from solar), substantially smoothing seasonal variability and strengthening grid reliability.

Some of the limitations of the study include:

i. No geotechnical survey was conducted; anchor design is preliminary.
ii. Water temperature profiles were not measured, so the cooling effect is estimated.
iii. Long-term degradation beyond PVsyst defaults was not modelled.

References

[1] National Control Center, "Nigeria Electricity System operator report," https://www.nsong.org/.

[2] I. I. Ozigis, R. A. Adeyemi, P. A. Ondachi, and S. O. Oodo, "Performance evaluation of Kainji hydro-electric power plant using artificial neural networks and multiple linear regression," *International Journal of Energy and Water Resources*, vol. 6, no. 2, pp. 231–241, Jun. 2022, doi: 10.1007/s42108-021-00135-3.

[3] A. Patil, G. Mamatha, P. S. Kulkarni, and A. Verma, "Analysis of Hybrid Floating Photovoltaic and Hydro-Power plant with HOMER Pro Software," in *10th IEEE International Conference on Power Electronics, Drives and Energy Systems, PEDES 2022*, Institute of Electrical and Electronics Engineers Inc., 2022. doi: 10.1109/PEDES56012.2022.10080502.

[4] D. Bhattacharya, "A Review of Hybrid Floating Solar Plant Designs," *Int. J. Res. Appl. Sci. Eng. Technol.*, vol. 11, no. 3, pp. 945–955, Mar. 2023, doi: 10.22214/ijraset.2023.49571.

[5] D. F. Silalahi and A. Blakers, "Global Atlas of Marine Floating Solar PV Potential," *Solar*, vol. 3, no. 3, pp. 416–433, Jul. 2023, doi: 10.3390/solar3030023.

[6] A Chiromo, O. Amu, C. Otonglo, and F. Balderamma, "Project Title: Kainji and Jebba Hydro Power Plant Rehabilitation Project."

[7] Global Solar Atlast, "www.globalsolaratlas.com," https://globalsolaratlas.info/map. Accessed: May 16, 2026. [Online]. Available: https://globalsolaratlas.info/map

[8] Google Earth, "www.google earth.com," Google Earth. Accessed: May 16, 2026. [Online]. Available: www.googlearth.com

[9] Q. Qin, Lukman Adeboye, Khalifa Aliyu Ibrahim, Patrick Luk, Ying Xie, Patrick Verdin, Zhenhua Luo, and Luofeng Huang, "Techno-economic and environmental assessment of floating solar power with innovative charging systems for decarbonizing maritime operations in the UK," *Renew. Energy*, vol. 256, Jan. 2026, doi: 10.1016/j.renene.2025.124398.

[10] B. Ou, B. C. Cerik, and L. Huang, "Seakeeping analysis of catamaran and barge floats for floating solar arrays: A CFD study with experimental validation," *Ocean Engineering*, vol. 326, May 2025, doi: 10.1016/j.oceaneng.2025.120970.

[11] PVsyst, "https://www.pvsyst.com/."

[12] D. M. Fouz, R. Carballo, I. López, B. Álvarez, and G. Iglesias, "Floating solar photovoltaic energy for coastal areas: A siting methodology," *J. Clean. Prod.*, vol. 528, Oct. 2025, doi: 10.1016/j.jclepro.2025.146733.

[13] A. T. Nedelcu, C. Faităr, I. Voicu, and M. Panaitescu, "Floating Photovoltaic Systems—Energy Performance and Environmental Challenges in Sustainable Development," *Sustainability (Switzerland)*, vol. 18, no. 5, Mar. 2026, doi: 10.3390/su18052588.

[14] M. Madeško, V. Helać, A. Fejzić, S. Konjicija, A. Akšamović, and S. Grebović, "Integrating Floating Photovoltaics with Hydroelectricity," *Energies*, vol. 17, no. 11, Jun. 2024, doi: 10.3390/en17112760.

[15] Zimmerman, "www.pv-floating.com." Accessed: May 17, 2026. [Online]. Available: www.pv-floating.com

Received: 17/05/2026; Revised: 23/05/2026; Accepted: 02/06/2026; Published: 27/06/2026